Supplementary Material for

Direct access to graphene-metal interface by Raman spectroscopy for study the origin of contact resistance in operational devices

Alessandro Kovtun[1]*, Leonardo Martini[2], Piera Maccagnani[3]*

[1] Consiglio Nazionale delle Ricerche, Istituto per la Sintesi Organica e la Fotoreattività, (CNR-ISOF), 40129 Bologna, Italy, [2]Dipartimento di Scienze Fisiche, Informatiche e Matematiche (FIM), Università di Modena e Reggio Emilia, 41125 Modena, Italy, [3] Consiglio Nazionale delle Ricerche, Istituto per lo Studio dei Materiali Nanostrutturati, (CNR-ISMN), 40129 Bologna, Italy.

* Corresponding authors: Alessandro Kovtun, alessandro.kovtun@cnr.it; Piera Maccagnani, piera.maccagnani@cnr.it

Content

Electrical Characterization

The DC characterization was carried out at wafer level in a Karl-Süss probe station, in ambient atmosphere (300 K, relative humidity of 40%), using four Keithley 238 (Keithley Instruments, Inc., Cleveland, OH, USA) source monitor units (SMU) connected to the probe through the switching matrix Keithley 707 (with 7072 and 7174 semiconductor cards).

Contact End Resistance (RCE) method

The TLM structures have been fabricated with two lithographic steps: the first step is for the patterning of the graphene structures, and the second one is for the definition of metal elements (contacts and pads). The extraction of ohmic contact parameters using TLM structures was performed plotting the total resistance R_T vs. the contact separation (L_{CH}), together with the R_{CE} measurements. The measurement setup used for the application of the CER method to the TLM test structures, is shown in Fig. SI 1. All the *I-V* measurements are linear (Fig. 1e) and R_T can be written as: [3]

$$R_T = \frac{V_{12}}{I_{12}} = R_{sh}\frac{L_{CH}}{W} + 2R_{CF} + 2R_M \quad [S1]$$

where R_{sh} is the sheet resistance of the graphene channel, R_{CF} is the contact front resistance related to the metal/graphene stack, and R_M is the series resistance due to the metal and can be neglected because $R_M \ll R_{CF}$. R_{CF} was obtained applying the extrapolation technique to R_T vs L_{CH} curve, as reported in the example in Fig. SI 2, where the measured R_T is reported for the different width of the graphene in the TLM structures.

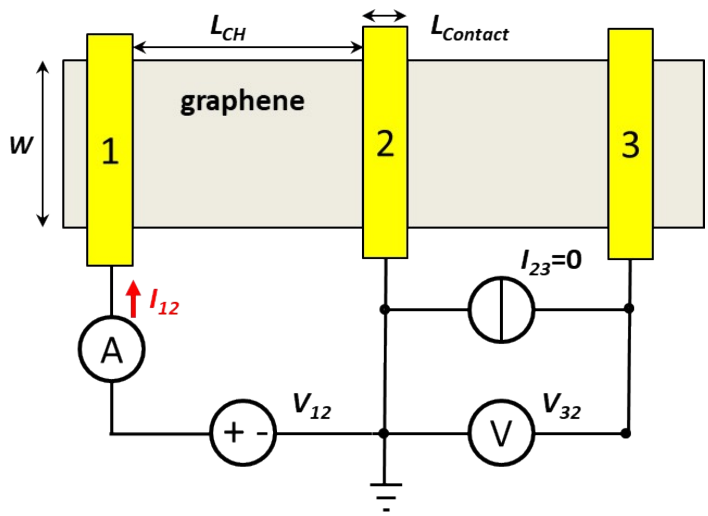

Figure S1. Measurement setup for TLM structures

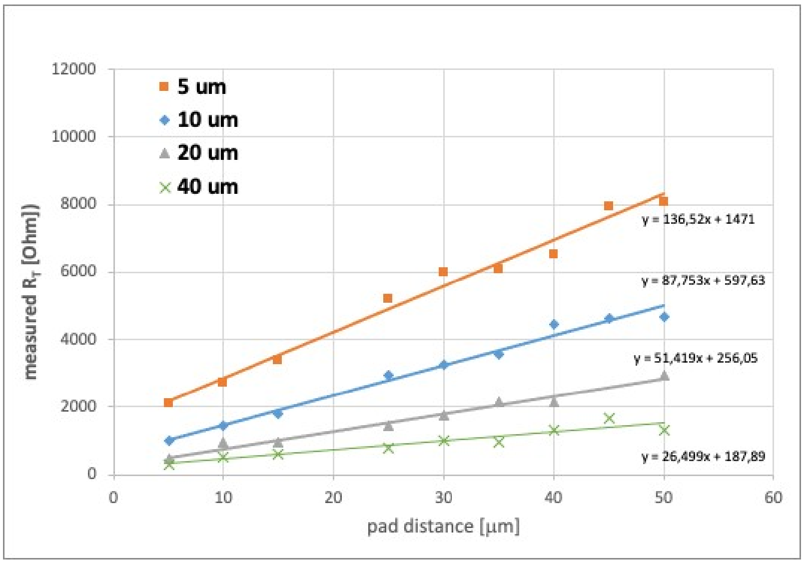

Figure S2. Plot of R_T vs. the pad distance, L_{CH}, for different width of the graphene stripe, *W*. The metal contacts are all 6 mm wide, while their length is the same as the graphene stripe (*W*). The slope of the fitting provides R_{SH}, and the intercept of the fitting straight line on the y-axis (R_T) provides the front-end contact resistance (2R_{CF}), while the intercept on the x-axis yields 2$L_{TK} \times (R_{SK}/R_{SH})$.

As explained in ref. [4], the contact front resistance R_{CF} can be modeled by means of a distributed *R-R* transmission line model, and neglecting the resistance related to the transport into the metal (for its very low metal resistivity), R_{CF} ca be shown to be equal to:

$$R_{CF} = \frac{R_{SK} \times L_{TK}}{W_{CH}} coth \frac{L_{CON}}{L_{TK}} \quad [S2]$$

where L_{TK} is expressed as:

$$L_{TK} = \sqrt{\frac{\rho_C}{R_{SK}}} \quad [S3]$$

To evaluate ρ_C the contact end measurement technique should be applied to TLM structures. [4] This method consists in imposing a null current between contacts 2 and 3 (I_{23} = 0) during the measurements of I_{12}, so that the voltage V_{32} drops across the metal/graphene stack at the border of contact 2 (where the current is vanishing), and the contact-end resistance can be expressed as:

$$R_{CE} = \frac{V_{32}}{I_{12}} = \frac{\rho_c}{L_{Tk} \times W_{CH}} \times \frac{1}{sinh(L_{CON}/L_{TK})} \quad [S4]$$

And exploiting eqs. [S2], [S3] and [S4] is obtained that:

$$\frac{R_{CF}}{R_{CE}} = \cosh\left(\frac{L_{CON}}{L_{TK}}\right) \quad [S5]$$

Therefore, using the experimental data for R_{CF} and R_{CE} and the equations above it's possible to extract the value for L_{TK}, ρ_C and R_{SK}. The values obtained are reported in Table 1 of the main paper.

Fig. SI 3 shows the experimental values extracted from CER measurements, for R_{CF} and R_{CE} as a function of the graphene width of the TLM structures (the reported data are averaged over several TLM structures). As expected from equations S2 and S4, both R_{CF} and R_{CE} scale inversely with W.

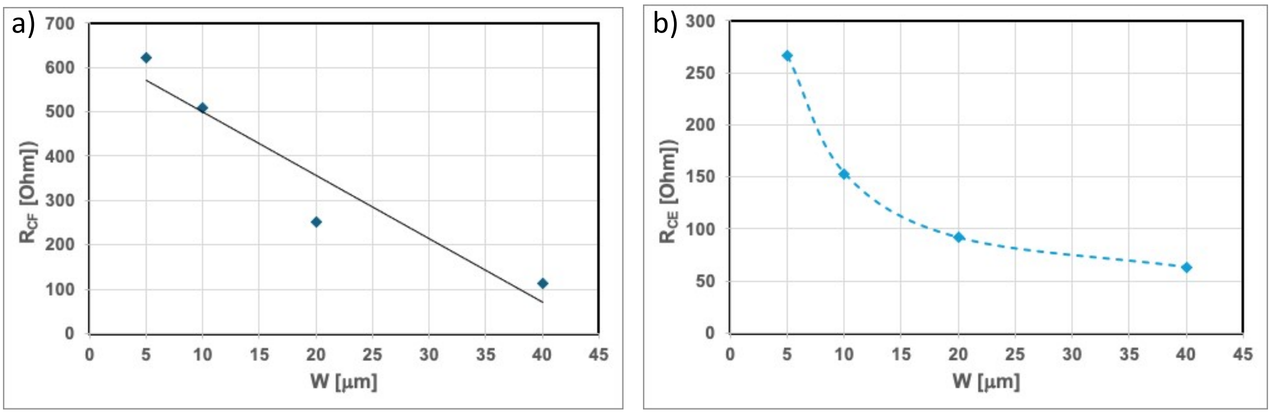

Fig. S3. (a) contact front resistance (R_{CF}) and (b) contact-end resistance (R_{CE}) as a function of the width of the graphene in the TLM structures.

Raman spectra and maps

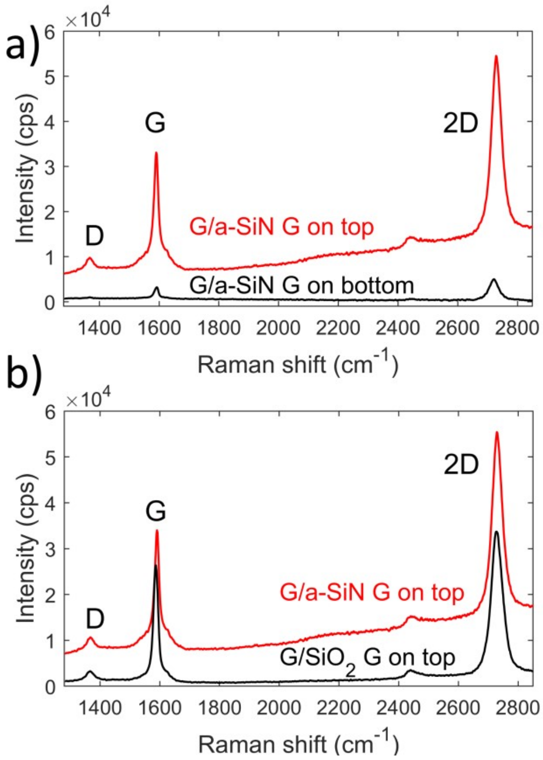

Figure S4. Representative Raman spectra for graphene on transparent substrate (G/a-SiN) with a) measurements performed on the top (conventional set-up, red curve) and with device flipped upside down (graphene on bottom, black curve); b) graphene on SiO_2 (black curve) and a-SiN (red curve).

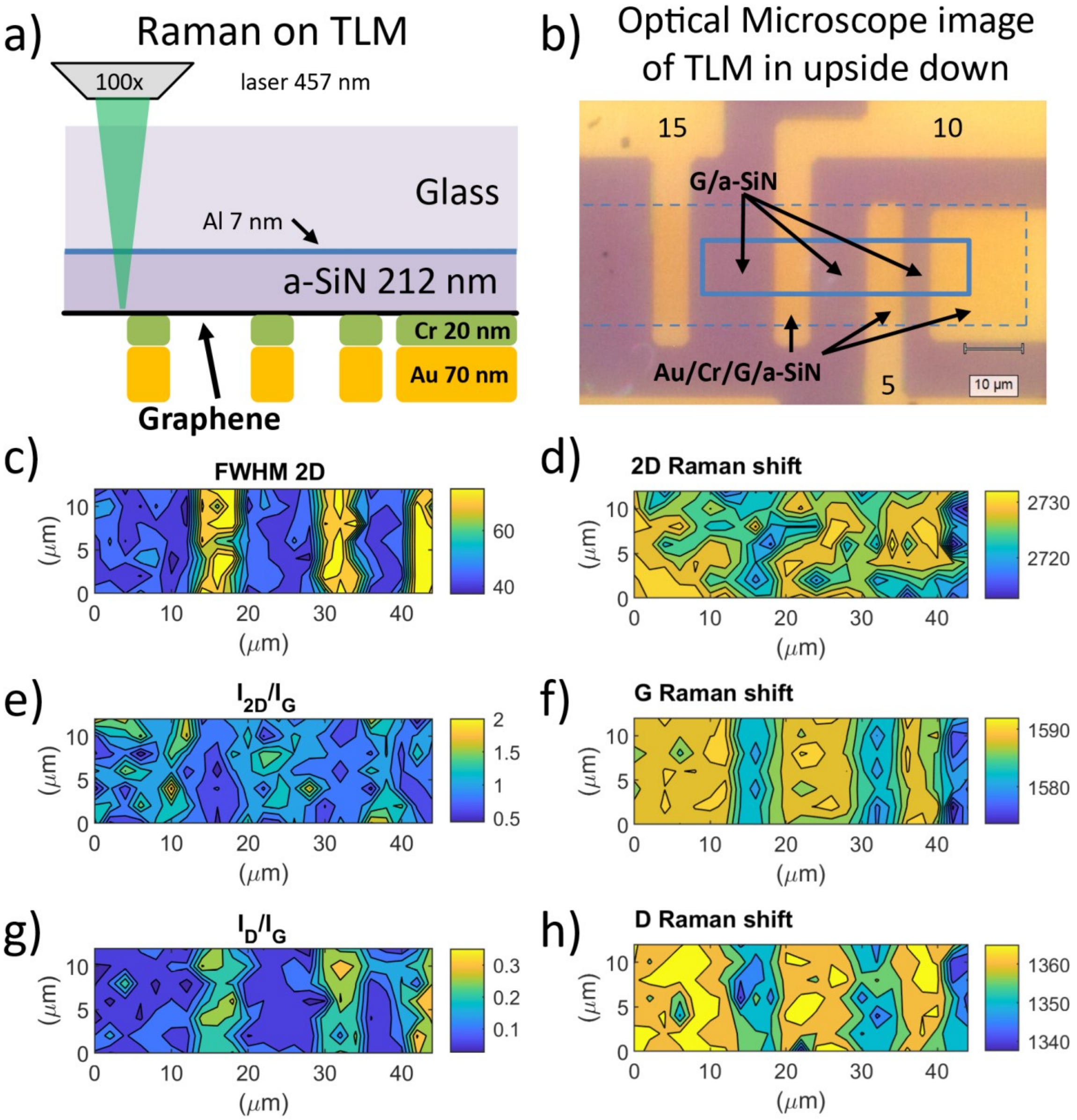

Figure S5. a) Scheme of the Raman measurement set-up of the graphene on transparent substrate and in upside down configuration, b) microscopy image of TLM test structure with 3 metallic contact (Au/Cr/G/a-SiN) separated by 3 channels (15, 10 and 5 µm channel length) where graphene is without metallic contact (G/a-SiN), the solid line rectangle represents the area of the sample probed by micro Raman, while the dashed lines underline the edges of the graphene; Raman maps of intensities of c) FWHM of *2D*, e) I_{2D}/I_G, and g) I_D/I_G. Raman maps of d) *2D*, f) *G* and h) *D* bands.

Bibliography

1. P. Maccagnani, Università di Ferrara, 2023 https://hdl.handle.net/11392/2506194.
2. A. J. Pollard, K. R. Paton, C. A. Clifford, and E. Legge, in *Good Practice Guide* (National Physical Laboratory, UK, 2017), Vol. 145.
3. S. Venica, F. Driussi, A. Gahoi, P. Palestri, M. C. Lemme, and L. Selmi, "On the adequacy of the transmission line model to describe the graphene–metal contact resistance", IEEE Transactions on Electron Devices **65** (4), 1589 (2018).
4. G. Reeves and H. Harrison, "Obtaining the specific contact resistance from transmission line model measurements", IEEE Electron device letters **3** (5), 111 (1982).